

First-principles calculations of Cs adsorbed on Cu(001): Quantum size effect in surface energetics and surface chemical reactivities

Bo Sun, Ping Zhang,* Suqing Duan, and Xian-Geng Zhao

Institute of Applied Physics and Computational Mathematics, P. O. Box 8009, Beijing 100088, People's Republic of China

Qi-Kun Xue

Institute of Physics, Chinese Academy of Sciences, Beijing 100080, People's Republic of China

(Received 18 January 2007; revised manuscript received 2 April 2007; published 20 June 2007)

First-principles calculations of Cu(001) free-standing thin films have been performed to investigate the oscillatory quantum size effects exhibited in surface energy, work function, atomic relaxation, and adsorption energy of a cesium adsorbate. Quantum well states have been identified and clarified at particular k points corresponding to the stationary extrema in the bulk Brillouin zone, and are in good agreement with experimental observations. The calculated surface energetics and geometry relaxations clearly feature quantum oscillations as a function of the film thickness, with oscillation periods characterized by a superposition of long and short length scales. Furthermore, we have investigated Cs adsorption onto Cu(001) thin films as a function of the film thickness. Our systematically calculated results clearly show large-amplitude quantum oscillations in adsorption energetics, which may be used to tailor catalysis, chemical reactions, and other surface processes in nanostructured materials.

DOI: [10.1103/PhysRevB.75.245422](https://doi.org/10.1103/PhysRevB.75.245422)

PACS number(s): 73.21.-b, 73.20.At, 73.21.Ac

I. INTRODUCTION

When the thickness of metal films approaches the nanoscale, oscillatory quantum size effects (QSEs) associated with electronic confinement and interference will occur¹⁻⁴ due to the splitting of the energy-level spectrum into subbands normal to the plane of the films, i.e., the quantum well (QW) states. These QW states lead to strongly modified physical properties and thus have been the subject of numerous investigations in recent years.^{5,6} For example, the QW states are found to be responsible for an unusual metallic film growth pattern,⁷⁻¹⁰ and for the thickness-dependent stability¹¹ observed in experiments. The QW states are directly connected to the oscillations in the exchange coupling between two magnetic materials across a nonmagnetic spacer layer of various thickness,¹² and to giant magnetoresistance.¹³⁻¹⁶ Moreover, the QW states also give rise to an oscillatory phonon-electron coupling as the film thickness varies, and thus affect the transition temperature to superconductivity.^{17,18}

Experimentally, the characterization of the QW states is commonly performed measured using angle-resolved photoemission spectroscopy (ARPES) and scanning tunneling microscopy (STM). ARPES can be used to study the band structure along any direction of the surface Brillouin zone (BZ), while STM offers the possibility to study local structures, such as islands, chains, dots, etc. Using the scanning tunneling spectroscopy (STS) technique, in which the differential conductance (dI/dV) is measured, one can further reliably determine the energy of quantized electronic states in the range of approximately 1 eV below and above the Fermi level. Theoretically, a number of approaches have been used in the past in order to describe the electronic properties, in particular the QW states, in ultrathin metallic films. Quasi-one-dimensional models, such as a square well potential¹⁹ or the phase accumulation model,²⁰ have been successfully used

to interpret the energies of QW states. More sophisticated methods such as the tight-binding approach²¹ and the layer-Korringa-Kohn-Rostoker approach^{22,23} have also been used. Recently, the QW states have been extensively investigated by self-consistent density-functional calculations.²⁴⁻³³ There are strong reasons to use the *ab initio* methods. First, there are no adjustable parameters, and the wide range of calculated structural and electronic properties offers the possibility of a detailed comparison with experiments. Also, quantities such as the expected STM profiles and the amplitudes of the wave functions of the QW states, which cannot be obtained in simple approaches, can be calculated within the *ab initio* treatment.

In this paper we report our first-principles calculations of the QSEs in a specific QW system, i.e., Cu(001) free-standing thin films. Previous QSE studies concerning Cu(001) mainly focused on the oscillations in magnetic interaction between the two ferromagnetic layers in fcc $M/\text{Cu}/\text{fcc } M$ (001) sandwich structures, where M denotes a ferromagnetic material such as Co. It has been demonstrated that the Cu(001) films have a long length scale of 5.6 monolayer (ML) and a short length scale of 2.6 ML of oscillation periods for magnetic coupling in the [001] direction, corresponding to spanning vectors at the belly and neck points of the bulk Cu Fermi surface, respectively.³⁴⁻³⁷ Recent experimental efforts have been focused on the new band structure properties of QW states in the Cu(001) system.³⁸⁻⁴⁶ On the other hand, the QSEs of Cu(001) associated with its energetics have scarcely been considered up to now. In particular, there is no clear experimental or theoretic evidence for the interplay between the different oscillation periods of Cu(001) films by the belly and neck extrema in the bulk Cu Fermi surface. Here we present a detailed first-principles study of the surface energetics of clean Cu(001) free-standing thin films. The QW states corresponding to the stationary extrema in the bulk BZ are fully studied. Quantum oscillations of the

energetics as a function of the thickness of Cu(001) films are identified, and the corresponding oscillation periods are clarified. We find that the quantum interference of the QW states with different in-plane wave vectors results in a superposition of long- and short-length oscillating periods.

The other purpose of this paper is to investigate the QSEs in surface adsorption energetics for a representative system in order to shed light on the effect of the QW states on the surface reactivities. Since the adsorption properties are typically characterized by the chemical bonding between the adsorbate and substrate surface, when the substrate is ultrathin, the QSEs in the substrate will also influence the behavior of the surface adsorption. Here we address a particular adsorbate system, i.e., Cs/Cu(001), as a case study to manifest the QSEs in surface adsorption properties. Due to its simple electronic structure and active chemical properties, which are intrinsic for alkali metals, Cs is a unique adsorbate on metal surfaces, and has been extensively studied. Concerning Cs adsorption on Cu metal surfaces, the recently published papers^{47–52} mainly focus on the investigation of electronic, dynamic, and geometric properties of Cs layers on Cu(111). The nature of the interaction between the Cs adatom and Cu(001) film has also been studied both via first-principles pseudopotential calculations⁵³ and through a jellium model approach.⁵⁴

Compared to the above mentioned work on Cs/Cu(001), our present emphasis is on QSEs in surface adsorption energetics, rather than giving a general overview of the nature of alkali-metal-atom adsorption on metal surfaces. In particular, although it has been well known that due to the charge redistribution between the adsorbed alkali-metal atom and the substrate,⁵⁵ the dependence of this charge redistribution on the thickness of the ultrathin substrate film is yet to be understood. We notice that there are emerging some high-quality experimental data for QSEs in metal surface reactivities. Aballe *et al.*⁵⁶ have observed quantum oscillations in the oxidation rate of ultrathin Mg(0001) films on W(110). Ma *et al.*⁵⁷ have observed quantum oscillations of O₂ adsorption and surface oxidation in ultrathin Pb mesas grown on Si(111) substrate. In particular, an experiment directly associated with the present Cs/Cu(001) system has been presented by Wu *et al.*,⁵⁸ who have clearly observed quantum oscillations in the adsorbate work function as a function of the film thickness. Further measurements related to the QSEs of the surface reactivities are expected to be systematically reported afterwards due to the availability of high-quality quantum metallic thin films. A thorough theoretical investigation of this aspect is necessary and will be helpful for experimental reference in the near future. Our results show that, in ultrathin Cu(001) films, the surface adsorption properties display well-defined QSEs.

This paper is organized as follows. In Sec. II, the *ab initio* based method and computational details are outlined. In Sec. III, the band structure and the properties of QW states at the belly and neck points in the bulk BZ are presented. In Sec. IV, the surface properties of clean Cu(001) films, including surface energy, work function, and interlayer relaxation as a function of the thickness of the films, are presented and discussed. In Sec. V, the adsorption properties of the alkali metal Cs on the Cu(001) surface are discussed in detail by

presenting the sensitivity of the adsorption energy to the thickness of the Cu(001) films. Finally, Sec. VI contains a summary of the work and our conclusion.

II. COMPUTATIONAL METHOD

The calculations were carried out using the Vienna *ab initio* simulation package⁵⁹ based on density-functional theory with projector augmented wave pseudopotentials⁶⁰ and plane waves. The free-standing Cu(001) films with the so-called repeated slab geometries were employed. This scheme consists in the construction of a unit cell of an arbitrarily fixed number of atomic layers identical to that of the bulk in the plane of the surface (defining the two-dimensional cell), but symmetrically terminated by an arbitrarily fixed number of empty layers (the “vacuum”) along the direction perpendicular to the surface. In the present study we have fixed the whole vacuum region equal to 20 Å, which is found to be sufficiently convergent. The two-dimensional unit cell of the fcc Cu(001) surface is a square of edge $a/\sqrt{2}$ with basis vectors $\mathbf{a}_1=(a/2)(1, \bar{1}, 0)$ and $\mathbf{a}_2=(a/2)(1, 1, 0)$ where a is the Cu bulk lattice constant. The corresponding surface BZ is a square with two high-symmetry directions $\bar{\Gamma}-\bar{M}$ and $\bar{\Gamma}-\bar{X}$. During our slab calculations the BZ integration was performed using the Monkhorst-Pack scheme⁶¹ with a $11 \times 11 \times 1$ k -point grid, and the plane-wave energy cutoff was set at 270 eV. Furthermore, the generalized gradient approximation (GGA) with the Perdew-Wang 1991 (PW-91) exchange-correlation potential has been employed with all atomic configurations fully relaxed. First the total energy of the bulk fcc Cu was calculated to obtain the bulk lattice constants. The calculated lattice constant is $a=3.639$ Å, comparable with the experimental⁶² value of 3.61 Å. The use of larger k -point meshes did not alter these values significantly. A Fermi broadening of 0.1 eV was chosen to smear the occupation of the bands around E_F using a finite- T Fermi function and extrapolating to $T=0$ K.

III. BAND STRUCTURE AND QUANTUM WELL STATES

We first studied the properties of electronic structures for bulk Cu and Cu(001) films. For this we used two kinds of unit cells of the crystal lattice; namely, unit cell I is defined via introducing the usual fcc basis vectors $\mathbf{a}_1=(a/2)(\mathbf{j}+\mathbf{k})$, $\mathbf{a}_2=(a/2)(\mathbf{i}+\mathbf{k})$, and $\mathbf{a}_3=(a/2)(\mathbf{i}+\mathbf{j})$, while unit cell II is defined by choosing Cu(001) as the basal plane, i.e., $\mathbf{a}_1=(a/2)(\mathbf{i}-\mathbf{j})$, $\mathbf{a}_2=(a/2)(\mathbf{i}+\mathbf{j})$, and $\mathbf{a}_3=a\mathbf{k}$. The volume of the second unit cell is twice that of the first one, and it is convenient to extend to the slab calculation since \mathbf{a}_3 is normal to the Cu(001) surface. Correspondingly, the reciprocal lattice basis vectors are $\mathbf{b}_1=(2\pi/a)(-\mathbf{i}+\mathbf{j}+\mathbf{k})$, $\mathbf{b}_2=(2\pi/a)(\mathbf{i}-\mathbf{j}+\mathbf{k})$, and $\mathbf{b}_3=(2\pi/a)(\mathbf{i}+\mathbf{j}-\mathbf{k})$ for unit cell I and $\mathbf{b}_1=(2\pi/a)(\mathbf{i}-\mathbf{j})$, $\mathbf{b}_2=(2\pi/a)(\mathbf{i}+\mathbf{j})$, and $\mathbf{b}_3=(2\pi/a)\mathbf{k}$ for unit cell II. Figure 1(a) shows the band structure and the density of states (DOS) of bulk fcc Cu (unit cell I). The highly dispersive s - p band, typical of noble metals, is present. The more intense d band region is located between 2.0 and 4.5 eV below the Fermi

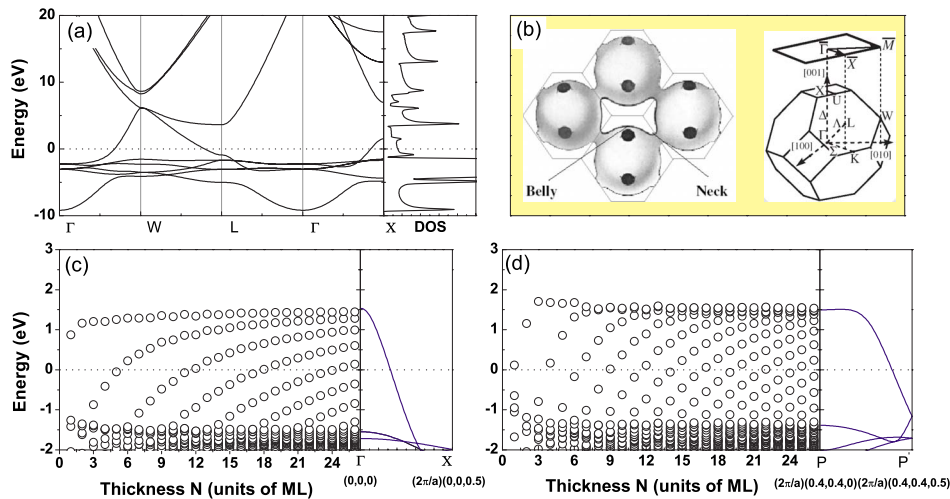


FIG. 1. (Color online) (a) GGA energy bands and density of electron states (right panel) of fcc bulk Cu with unit cell I (see the text). (b) The Cu Fermi surface showing the belly and neck regions. The bulk and surface BZs are also depicted. (c) Calculated (GGA) energies at $\bar{\Gamma}$ in Cu(001) thin films as a function of thickness, with the energy set to zero at the Fermi level. The right panel plots the bulk (with unit cell II) energy dispersion in the [001] direction. (d) Calculated (GGA) energies at \bar{P} in Cu(001) thin films as a function of thickness, with the energy set to zero at the Fermi level. The right panel plots the bulk (with unit cell II) energy dispersion in the [001] direction. The dotted line denotes the Fermi level.

surface and can be measured by a large rise of the intensity in photoemission experiments.¹² The *s-d* hybrid band region with two less intense dispersive states can also be seen in Fig. 1(a). The Fermi surface of bulk Cu and the Brillouin zone for unit cell I are schematically shown in Fig. 1(b). Of particular interest for Cu(001) thin film studies are the two extremal points, i.e., the belly and neck points of the bulk Fermi surface. Previous extensive studies have shown that stationary spanning vectors connecting the belly and neck points, respectively, play a key role in determining the oscillatory behavior of the interlayer magnetic exchange interaction $J_{M/M}$ in fcc $M/\text{Cu}/M$ (001) sandwich structures, where M denotes the ferromagnetic material. The belly extremum was found to correspond to a long oscillating period in $J_{M/M}$ while the neck extremum corresponds to a short period.

One inconvenience in discussing properties of Cu(001) films via the bulk Fermi surface calculated from unit cell I lies in the fact that none of the three basis vectors of unit cell I is normal to the (001) surface, which leads to an oblique projection of the bulk BZ onto the (001) surface BZ. On the contrary, by use of unit cell II, the discussions, particularly for QW states of (001) thin films, become very convenient. Beginning with this unit cell construction, the belly point in the bulk BZ is still projected to the $\bar{\Gamma}$ point, as with unit cell I, whereas the neck point, after projection, is at the $\bar{\Gamma}X$ line. In this paper the neck point will be named P and \bar{P} for bulk and surface BZ (with respect to unit cell II), respectively. Our band structure calculation gives the position [in coordinates of (k_x, k_y, k_z)] of P to be $(2\pi/a)(0.4, 0.4, 0.0)$.

Now we turn to study the electronic structure of Cu(001) thin film with focus on QW states. Since previous studies¹² have shown that the long and short oscillating periods in the interlayer magnetic exchange interaction originate from the band dispersions at the $\bar{\Gamma}$ and \bar{P} points, respectively, we ex-

pect the other intrinsic film properties such as film energetics, atomic structure relaxations, and even surface chemistry to be closely related with the QW states at these two kinds of stationary k points. Figure 1(c) shows the energies of the QW states at the $\bar{\Gamma}$ point as a function of the film thickness without interlayer relaxation. The energy zero is set at the Fermi level of each film. The interlayer relaxation effect is also studied and it is found that the overall thickness dependence of the energies is similar to that without relaxation. For comparison, also plotted in Fig. 1(c) (right panel) is the energy dispersion in the bulk along the [001] ($\Gamma \rightarrow X$) direction, which corresponds to the center $\bar{\Gamma}$ of the (001) surface BZ and determines the energy range for the QW states shown in the left panel. One can see from Fig. 1(c) that, as the thickness of the film increases, the energy of a given QW state also increases. When the thickness of the film is increased to be about 5.0 monolayers, then a QW state, with the energy crossing the Fermi level, occurs. The next energy crossing with the Fermi level occurs at the film thickness of ~ 11 monolayers. Our calculated result for quantum well states is in good agreement with the recent experimental ARPES measurement,¹² in which the photoemission intensity as a function of energy for fixed Cu thickness and as a function of Cu thickness for fixed energy clearly showed the existence of the QW states of the *sp* electrons in the Cu layer. Figure 1(d) shows (left panel) the energies of the QW states at the \bar{P} point as a function of film thickness without interlayer relaxation. The energy zero is set at the Fermi level of each film. Again the bulk energy dispersion along the [001] direction (starting from the P point) is also shown in Fig. 1(d) (right panel). One can see that, for every incremental increase in the film thickness of about 2.7 ML, a new quantum well state crosses the Fermi level. A comparison between the left and right panels in Fig. 1(c) [or Fig. 1(d)] shows that the bulk

electron band of Cu works very well for QW states as when the Cu thickness is greater than 5 ML, which agrees well with the experimental results.⁶³

Quantitative understanding of the QW states showed in Figs. 1(c) and 1(d) is usually obtained using the so-called phase accumulation model.^{64–66} Here the free-standing Cu(001) film is considered as a QW confining electrons between the two vacuums in the slab. Since the system is invariant on translation parallel to the (001) plane, the in-plane wave vector $\mathbf{k}_{\parallel} \equiv (k_x, k_y)$ is a good quantum number. Thus, for a given \mathbf{k}_{\parallel} , the quantization condition for an electron state in such a well is given by

$$2k_n^{\perp}Nd + 2\phi = 2\pi n, \quad (1)$$

where N is the number of atomic layers in the film, $d=a/2$ is the interlayer spacing, ϕ is the phase gain of the electron wave function upon reflection at the the film-vacuum interface, n is the number of half-wavelengths confined inside the QW, and k_n^{\perp} describes the Cu electron wave vector component along the [001] direction for the n th QW state. Equation (1) has been successfully used to model QW states in metal thin films, and its validity has been rigorously tested by full-scale first-principles calculations for some special systems.²⁹ It should be addressed that QW states will not only form at the $\bar{\Gamma}$ point but also form in a large part of the surface BZ, and the quantization condition (1) may be applied throughout the entire zone. Using Eq. (1) one can calculate the periodicity for the QW states crossing the Fermi level, $\Delta N = \pi/[k_F^{\perp}(\mathbf{k}_{\parallel})d]$, where $k_F^{\perp}(\mathbf{k}_{\parallel})$ is the bulk Fermi wave vector along the [001] direction for a given in-plane wave vector \mathbf{k}_{\parallel} . For the $\bar{\Gamma}$ point ($\mathbf{k}_{\parallel}=\mathbf{0}$), from the right panel in Fig. 1(c), one can see that the upper branch of the bulk sp band runs through $\sim 36\%$ of the BZ, $k_{\perp}^f \approx 0.36\pi/c$. One gets $\Delta N \approx 5.6$. Therefore a new QW state of $\mathbf{k}_{\parallel}=(0,0)$ occurs for every 5.6 ML increase of the film thickness. It is verified in the left panel in Fig. 1(c) that an energy branch moves down, crossing the Fermi level for every incremental increase in the film thickness of six layers. Similarly for the \bar{P} point corresponding to $\mathbf{k}_{\parallel}=(2\pi/a)(0.4,0.4)$ in the bulk BZ, one can derive from the right panel in Fig. 1(c) $k_{\perp}^f \approx 0.75\pi/c$. In this case, Eq. (1) gives the periodicity for the QW states to be $\Delta N \approx 2.7$. Therefore, Figs. 1(c) and 1(d) reveal that the periodic behavior of the Cu(001) QW states is essentially governed by the bulk Cu electronic structure properties. In particular, the extremal points of the Fermi surface and the extremal points of the QW branches close to the Fermi level occur at the same \mathbf{k}_{\parallel} , i.e., at $\mathbf{k}_{\parallel}=(0,0)$ in the bulk BZ corresponding to $\bar{\Gamma}$ in the (001) surface BZ, and for the neck extremum $\mathbf{k}_{\parallel}=(2\pi/a)(0.4,0.4)$ both in the bulk and in the surface BZ. This relation between the Fermi surface and the quantum well dispersion turns out to be very fruitful for the understanding of the connection between the periods in energetics and surface reactivities discussed below.

The energies of QW states near the Fermi level can be measured by STS experiments, in which the local density of states is probed through the dI/dV curve. The distinctive sharp peaks in the dI/dV curve are characteristic of the QW

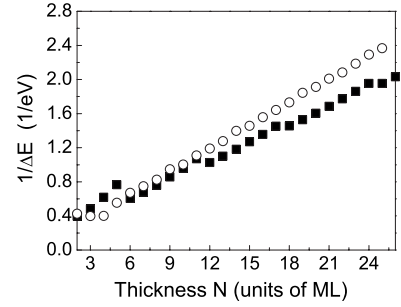


FIG. 2. Inverse of the energy gap between the highest occupied QW state and the lowest unoccupied QW state as a function of Cu(001) film thickness. The squares in the figure are the results for the $\bar{\Gamma}$ point in the surface BZ, while the circles are for the \bar{P} point [projection of the bulk Fermi surface's neck onto the (001) plane].

states at different quantum numbers. The easiest quantity to see in STS measurements is the energy gap ΔE between the highest occupied QW state and lowest unoccupied QW state. To see the thickness dependence of ΔE , taking the derivative of Eq. (1) with respect to energy and evaluating it at the Fermi level for a given N , one has²⁹

$$\frac{1}{\Delta E} \approx \frac{2d}{\hbar v_F} N + \frac{1}{2\pi} \phi'(E_F), \quad (2)$$

where v_F is the Fermi velocity obtained from the slope of the bulk band at the Fermi level and $\phi'(E_F)$ the energy derivative of the interface electronic phase shift at the Fermi level. Therefore, the measured $1/\Delta E$ curve is a linear function of N , with a slope connected to v_F . Figure 2 shows the calculated $1/\Delta E$ at the $\bar{\Gamma}$ and \bar{P} points using the QW energies in Figs. 1(c) and 1(d). One can see that the two curves follow a straight line with different slopes. Also it can be seen that, when a new branch of QW states crosses the Fermi level, a kink occurs. Due to the different periods at $\bar{\Gamma}$ and \bar{P} , the kinks in these two curves are also located at different values of N . Note that the intersection of the linear curves with the horizontal axis is not necessarily at $N=0$, due to the nonzero energy derivative of the interfacial phase shifts at the Fermi level.³⁰

Another central quantity closely related to the above discussed QW electronic structure of the Cu(001) thin film is the film electronic DOS at the Fermi level, $D(E_F)$. As shown in Fig. 3, the film $D(E_F)$ with respect to the film thickness displays well-defined oscillations with oscillation periods characterized by a superposition of long and short length scales. Note that in obtaining Fig. 3 we have increased the k grid for integration to $25 \times 25 \times 1$ for each value of N , which ensures the precision of the result. The oscillations in $D(E_F)$ give a periodic band energy contribution to the total energy, thus producing oscillatory surface energetics and reactivities which will be shown below.

IV. FILM ENERGETICS AND INTERLAYER RELAXATION

An energetic quantity suitably tailored to the QSE is the surface energy E_s , which is defined as one-half of the energy

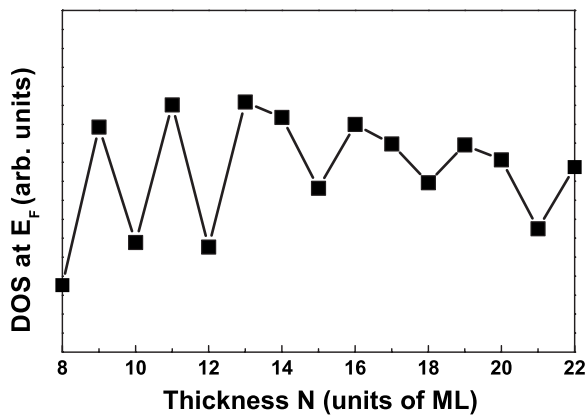


FIG. 3. Calculated electronic density of states at the Fermi energy as a function of Cu(001) thin film thickness.

(per surface atom or per 1×1 surface area) difference between the film and the reference bulk with the same number of atoms. Here the reference bulk total energy is, as suggested in Ref. 67, obtained in this paper by a linear fitting of the slab total energies. The resultant calculated thickness dependence of surface energy is shown in Fig. 4 (curve with squares). It reveals that the surface energy approximately follows a periodic oscillatory form, in accord with the oscillation properties of the film, $D(E_F)$. This can be simply reasoned by the fact that the total band energy with respect to the Fermi level is related to the DOS by the equation $E_{\text{band}} = \int^{E_F} (E - E_F) D(E) dE$. Therefore, the periodic crossings between the QW states and the Fermi energy will result in oscillations in $D(E_F)$, which in turn leads to a periodic change in band energy and produces an oscillatory behavior in the surface energy as a function of the film thickness. In the same manner as discussed above, one can expect that the oscillations in the surface energy consist of a superposition of oscillations with the periods corresponding to the extremal points of the bulk Fermi surface. To illustrate this, also plotted in Fig. 4 [red (gray) curve] is a least-squares fit to the surface energy with the following expression:

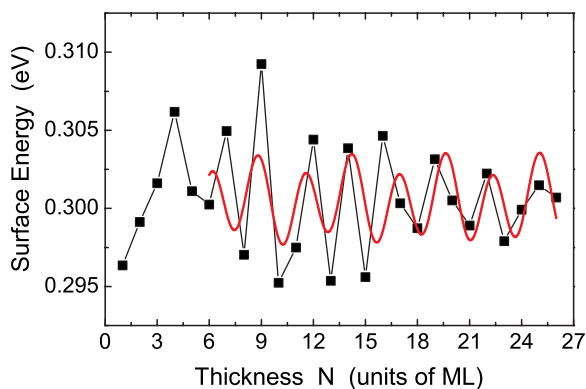


FIG. 4. (Color online) Surface energy for fully relaxed Cu(001) 1×1 slabs as a function of thickness. The red (gray) curve is a least-squares fit to the surface energy.

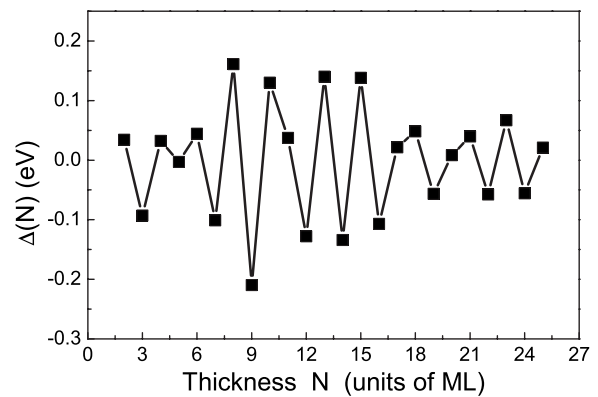


FIG. 5. Second difference of the total energy as a function of thickness for free-standing Cu(001) thin films.

$$E_{\text{surf}}(N) = \sum_{i=1}^2 A_i \sin\left(\frac{2\pi N}{\Lambda_i} + \phi_i\right), \quad (3)$$

where N is the number of monolayers, $\Lambda_1=5.6$ and $\Lambda_2=2.7$ are the periodicities (in unit of atomic MLs) corresponding to the belly and neck extrema in the bulk Cu Fermi surface, and A_i and ϕ_i are the fitting parameters. It can be seen that the fitting curve well reproduces the oscillating behavior in the surface energy, which again indicates that the stationary extrema in the Fermi surface play a key role in determining the oscillatory behavior in surface energetics.

Some authors have used the energies of the QW states at $\bar{\Gamma}$ to discuss the stability of the film. See Ref. 30 for an example. The key point employed there is that, even though the confinement takes place only in one of the three dimensions, the stability of the film could also be affected due to the variation in the electronic energy.⁶⁸ In the present case, since the above discussions have clearly shown that the neck point P in the bulk Fermi surface plays the same important role as the belly point (corresponding to $\bar{\Gamma}$ in the surface BZ) does in determining the oscillatory energetics properties of Cu(001) thin films; thus one can reasonably expect that the stability of the film also exhibits a superposed oscillatory behavior as a function of the film thickness, with the oscillation periods consisting of long and short length scales. To illustrate this, following Ref. 30, we use the second difference of the total energy as a measure of the relative stability of an N -layer film with respect to the films of $N+1$ and $N-1$ layers,⁶⁹ which is defined by

$$\Delta(N) = E(N+1) + E(N-1) - 2E(N), \quad (4)$$

where $E(N)$ is the calculated total energy of the fully relaxed N -layer film. The result is shown in Fig. 5. A peak in the figure indicates a high relative stability for the film. It is not surprising that the stability is featured by a superposition of long- and short-period oscillations as is evident from the above discussions. Remarkably, one can see that the $N=8$ film is mostly stable while the $N=9$ film is particularly unstable.

In addition to the surface energy, we have also calculated the work function W of free-standing Cu(001) thin films. The

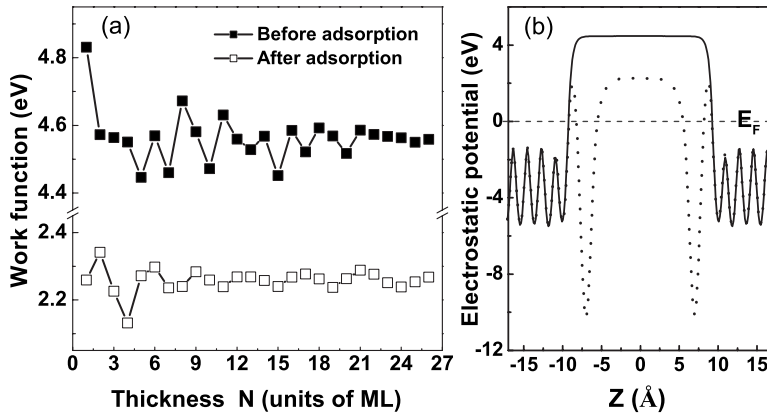


FIG. 6. (a) Work function for clean and Cs-adsorbed Cu(001) thin films as a function of thickness. (b) Planar-averaged electrostatic potential of clean (solid curve) and Cs-adsorbed (dotted curve) Cu(001) thin film (ten-layer Cu slab).

work function, defined as the minimum energy required to emit an electron from the surface to the vacuum, is one fundamental physical quantity for surface reactivity. An elementary picture of the work function involves a surface dipole layer that a valence electron must overcome in order to escape. Since the work function, as with many other properties, is also a function of the electronic density, thus the changes in the electronic density by the crossings between the QW states and Fermi level will influence the work function in an oscillatory way. In addition to its relevance as an important element in our understanding of surface science, a modified, or tunable, work function can be useful for applications such as catalysis, because a slight change in the energy scale is exponentially amplified for chemical reactions.⁷⁰ Recent *in situ* experiments have measured atomic-layer-resolved work function and shown clear QSEs in Ag/Fe(100) (Ref. 71) and Pb/Si(111) (Ref. 57) systems. Here we have carried out first-principles calculations of the work function of the clean Cu(001) surface. The result is shown in Fig. 6(a) (filled squares) as a function of film thickness with relaxed atomic geometry. One can see that the work function is featured by an oscillatory behavior. As with the surface energy, the oscillations in the work function of Cu(001) thin films consists of a superposition of long- and short-length periods.

In addition to the film energetics discussed above, the relaxed atomic structures of the Cu(001) thin film will also be influenced by the occurrence of QW states at the Fermi level. Since 1×1 supercells are employed and \mathbf{k}_{\parallel} is a good

quantum number, only atomic interlayer relaxation along the [001] direction is allowed during our calculations. Here the interlayer relaxation $\Delta d_{i,i+1}$ is given in percentages with respect to the unrelaxed interlayer spacings d_0 , i.e., $\Delta d_{i,i+1} = 100(d_{i,i+1} - d_0)/d_0$. $d_{i,i+1}$ is the interlayer distance between two adjacent layers parallel to the surface calculated by total energy minimization. $d_0 = a/2$ is the bulk interlayer distance along the [001] direction. Obviously, the signs + and - of $\Delta d_{i,i+1}$ indicate expansion and contraction of the interlayer spacings, respectively. The interlayer relaxations of Cu(001) films as a function of the film thickness are summarized in Table I. Furthermore, the interlayer relaxations are also plotted in Fig. 7 as a function of N for clear illustration. One can see the following (i) The two outmost layers relax significantly from the bulk value, in agreement with the result from full-potential linear augmented plane-wave calculation.⁷² In the whole range of layers that we considered, the topmost interlayer relaxation is always inward ($\Delta d_{1,2} < 0$), with $\Delta d_{1,2}$ starting from the largest value of -5% for a slab with only two monolayers, and approaches a final value of -3% with increasing thickness of the Cu(001) films, whereas, the second interlayer relaxation is always outward ($\Delta d_{2,3} > 0$). Note that the first interlayer separation on most metal surfaces is contracted; Cu(001) is a typical examples. (ii) The interlayer spacings oscillate as a function of the film thickness with the period again consisting of long and short length scales. After 26 monolayers, which is the maximal number of layers considered here, the oscillations are invisible, suggesting that the semi-infinite surface limit is now reached.

TABLE I. Interlayer relaxations (%) $\Delta d_{i,i+1}$ of Cu(001) as a function of the thickness of the film.

N	Δd_{12}	Δd_{23}	Δd_{34}	Δd_{45}	Δd_{56}	Δd_{67}
2	-5.186					
3	-3.351	-3.350				
4	-3.131	+0.616	-3.144			
5	-3.425	+0.081	-0.099	-3.431		
6	-2.798	+0.477	-0.213	+0.487	-2.800	
7	-4.076	+0.126	+0.398	+0.394	-0.115	-4.066
8	-2.693	+0.189	-0.320	-0.066	-0.317	+0.185
9	-2.917	+0.369	+0.133	+0.484	+0.492	+0.134
10	-3.358	+0.343	-0.364	+0.039	-0.335	-0.042

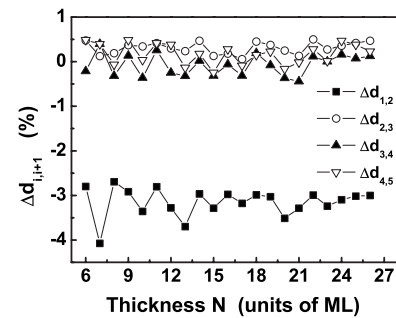


FIG. 7. Interlayer relaxations of Cu(001) thin films as a function of the film thickness.

V. ADSORPTION OF CESIUM: QSE IN SURFACE CESIATION

In the above discussions we have extensively studied the QW states in Cu(001) thin films and corresponding QSEs in various physical quantities such as surface energy, work function, and interlayer relaxations. To further illustrate the physical properties influenced by the finite-size effect of the thin films, in this section we focus our attention on the adsorption of Cs on Cu(001) thin films. Note that our study in this section is not just for an alternative verification of QSEs in solid thin films. On the contrary, the present study of surface adsorption as a function of film thickness has its own cause to be emphasized. It is well known that metal surfaces are a prototype heterogeneous catalyst, and have been widely studied in terms of the dissociative chemisorption of the reactant molecules. For a given solid, except for surface irregularities such as steps and defects, its surface reactivity is almost solely determined by the crystallographic orientation. At reduced size and/or dimensionality, particularly when the characterized size enters the nanometer scale, however, the situation could be dramatically different from that of the bulk. In fact, size-dependent surface chemical activities in metal films with thickness of the nanometer scale have been observed in previous experimental reports.^{56,73} Remarkably, in a very recent oxygen adsorption experiment on high-quality Pb(111) thin films, Ma *et al.* have clearly observed an oscillatory dependence of the chemical reactivity on the film thickness,⁵⁷ thus providing a most convincing proof of the key role played by the QW states in changing surface reactivity. It is expected that more experiments will address the issue of QSE in surface chemical reactivity. Therefore, the present detailed theoretical analysis for the dependence of the behavior of Cs adsorption upon the Cu(001) film thickness is very interesting.

Before we study the Cs adsorption properties as a function of the thickness of Cu(001) thin films, we need to determine the energetically favorable adsorption site. Since the preference for the adsorption site is not sensitive to the thickness of the substrate, to look for this preferred adsorption site, it is sufficient to study slabs with fixed thickness of the Cu(001) substrate, which is at present chosen to be 5 ML. We choose the four most probable adsorption sites, which is enumerated in Fig. 8. The binding energy is calculated using the following equation: Binding energy (atomic Cs) = $-\{E[\text{Cs}/\text{Cu}(011)] - E[\text{Cu}(001)] - 2E(\text{Cs})\}/2$ where $E[\text{Cs}/\text{Cu}(001)]$ is the total energy of a slab which includes two Cs atoms inside with a symmetric configuration, $E[\text{Cu}(001)]$ is the total energy of the slab without Cs atoms, and $E(\text{Cs})$ is the total energy of a free Cs atom in a $16 \times 16 \times 16 \text{ \AA}^3$ supercell. The calculated Cs/Cu(001) binding energies are 0.9189, 0.9176, 0.9174, and 0.9327 eV for sites 1, 2, 3, and 4 respectively. Thus site 4 is most stable for adsorption. This is in accord with recent experiments that for substrate surfaces with square or rectangular symmetry the alkali-metal atoms occupy adsorption sites which maximize the coordination number to the substrate.^{74–80} Thus in the following the atomic Cs is always put on site 4 during the simulation. This adsorption site is independent of the cover-

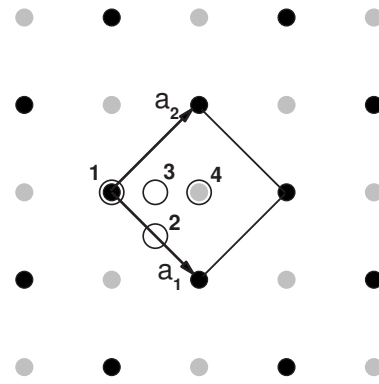


FIG. 8. Four different adsorption sites for the Cs adatom on a Cu(001) surface. The Cs adatoms and Cu atoms in the topmost surface layer are indicated by open circles and black circles, respectively, while the second-layer Cu atoms are depicted as gray circles.

age Θ of Cs atoms. In this paper, we consider only the case of $\Theta=0.5$.

To illustrate the surface bond formed between the Cs adatom and Cu surface atoms, we depict in Fig. 9(a) the contour map of the electron-density difference for Cs/Cu(001). Here the plane depicted is normal to the surface and contains a Cs and two Cu atoms. The density difference is obtained by subtracting the densities of noninteracting component systems, $\rho[\text{Cu}(001)] + \rho(\text{Cs})$, from the density of the Cs/Cu(001) system, $\rho[\text{Cs}/\text{Cu}(001)]$, while retaining the positions of the component systems at the same location as in Cs/Cu(001). Covalent bonding is evident from the accumulation of the charge between the Cs adsorbate and the Cu(001) substrate. This charge is drawn principally from the atomic 6s state of the Cs adlayer. On the vacuum side of the overlayer the charge is depleted. Thus the Cs 6s state causes a polarization toward the Cu(001) surface. As a response, the

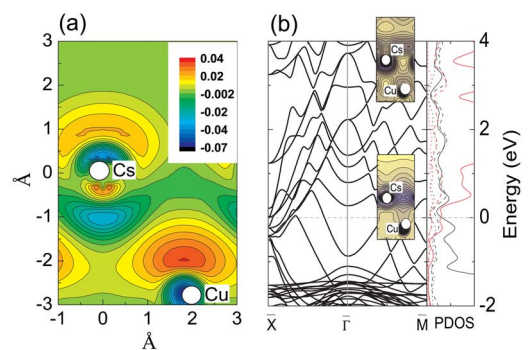


FIG. 9. (Color online) (a) Contour plot of charge density difference, $\rho[\text{Cs}/\text{Cu}(001)] - \rho[\text{Cu}(001)] - \rho(\text{Cs})$, in the (100) plane, for the cesiated Cu(001) surface. (b) (Left panel) Band structure of cesiated Cu(001) thin film (five-layer Cu slab) with coverage $\Theta=0.5$; (right panel) decomposition of local DOS for Cs adatom [red gray curves] and surface Cu atom (black curves) into states with *s* (dotted curves), *p* (dashed curves), and *d* (solid curves) character for the Cs/Cu(001) system. The inset in (b) predicts the band charge densities around the Fermi level (lower panel) and above the Fermi level (upper panel) of typical value of 3.5 eV.

work function will be decreased by this occurrence of surface polarization. On the other side, a significant *counterpolarization* of the Cs $5p$ semicore charge is also quite evident from Fig. 9(a). This effect opposes the reduction of the work function and the ultimate value of work function represents a self-consistent compromise between $6s$ and $5p$ polarization. The net result of these multiple surface dipoles, as shown in Fig. 6(b), is a lowering of the work function upon cesiation from 4.473 eV [clean ten-layer Cu(001) slab] to 2.259 eV for the coverage $\Theta=0.5$, corresponding to the relaxed height of the Cs atom above the Cu film of 2.988 Å. Also due to this opposite orientation between $6s$ and $5p$ polarization, the work function of Cs/Cu(001) displays a nonmonotonic variation with increasing coverage of Cs: At low coverage, the work function decreases with increasing coverage, going through a minimum (at about $\Theta=0.5$), and increases a little bit from there to the high coverage value.⁸¹ A similar picture of the cesiation process also been largely discussed in the Cs/W(001) system.⁸² A well-known conclusion in studying alkali-metal-atom chemisorption onto a metal surface is that, although the region around the alkali-metal adatom is electrically neutral and no net charge transfer toward the metal surface is exhibited, the electrons of the alkali-metal adatom undergo a strong mixing with the substrate electron orbitals during the adsorption process. Such a process is local around the adatom and accompanied by a screening process, which is responsible for work function change. Furthermore, Fig. 9(b) shows the band structure (left panel) and the orbital-resolved local DOS (right panel) for the Cs adatom and surface Cu atom, respectively. The complex Cs-induced charge rearrangement is more obvious. The Cs adatom experiences during adsorption a repulsive interaction of the valence electron with the induced image charge of the ionic nuclear core. As a result, the valence electrons shift upward in energy and hybridize with those of the substrate into bonding and antibonding states.^{83,84} The bonding states are mainly around the Fermi level and are dominated by hybridization between adatom sp and surface Cu sp orbitals, as shown in the lower panel in the inset in Fig. 9(b); whereas the antibonding states shift up away from the Fermi level with a typical value of 3.8 eV, and largely consist of hybridization between Cu s and Cs d orbitals, which can be seen from the upper panel in the inset in Fig. 9(b). A thorough description of the bonding properties in Cs/Cu(001) system is beyond our intention in this paper.

After finding the preferred atomic Cs adsorption site (site 4 in Fig. 8) and getting familiar with the Cs-Cu(001) bonding properties, we turn now to our central focus on the QSEs in surface chemisorption and reactivity. For this purpose, we have given a series of calculations for the binding energy (the reverse of the adsorption energy) of the Cs adsorbate as a function of the thickness of Cu(001) thin films. Here as mentioned above we only consider the case of $\Theta=0.5$. The results are depicted in Fig. 10(a). One can see that the binding energy of Cs onto Cu(001) thin films depends on the film thickness in a damped oscillatory way. These oscillations are featured by a superposition of long- and short-length periods, thus indicating a well-defined QSE in the surface chemical reaction of Cu(001) thin film with respect to Cs adsorption. In experiment this QSE of atomic adsorption can be ob-

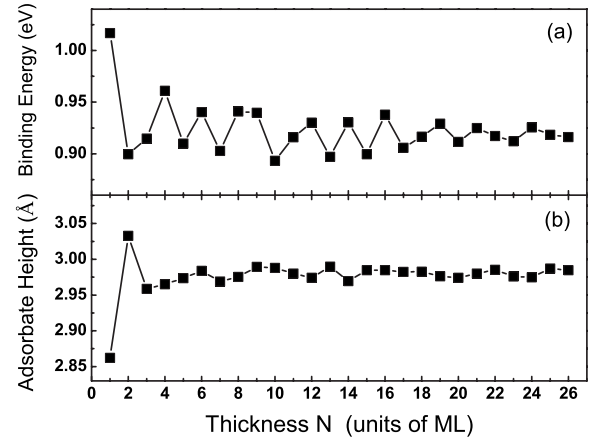


FIG. 10. Calculated (a) binding energy of Cs adatom and (b) adsorbate height as a function of thickness of the Cu(001) films.

served by investigating the dependence of Cs coverage on the monolayers of Cu(001) thin films. We note here that the calculated data in Fig. 10 have been carefully checked. This ensures that the oscillating behavior of the adsorption energy has nothing to do with the convergence problem, which may be encountered in the cluster calculations. The supercell approach retains two-dimensional 2D periodic boundary conditions during calculation, and can avoid this problem. Therefore, as with other quantities, the oscillations in adsorption energy are physically caused by the periodic change in the DOS at E_F . In fact, from what we have shown in Figs. 9, or from the simplest Anderson-Grimsley-Newns adsorption model,^{85,86} one recalls that as a Cs atom approaches to the Cu(001) surface (which can be approximated by a free-electron-like metal), the valence s - p states of Cs adatom are broadened into resonant states as a result of interaction with the metal bands. The surface electrostatic potential will shift this hybridization down in energy to below E_F to sustain the whole neutralization. A lower DOS at E_F implies that the Cu(001) film has fewer electronic states to respond, whereas a higher $D(E_F)$ means that the film has more electronic states to respond to the presence of the Cs adsorbate. Therefore, higher $D(E_F)$ implies higher probability in the above hybridization process, causing the sp resonance to move to lower energies and to be occupied. This leads to a higher surface reactivity and higher adsorption energy. The above physical picture can be formulated by expressing the adsorption energy as

$$E_{\text{ad}} = E_{\text{band}}(\text{unadsorbed}) - E_{\text{band}}(\text{adsorbed}) \approx \int_{-\infty}^{E_F} E \Delta D dE, \quad (5)$$

where $E_{\text{band}}(\text{unadsorbed})$ is the band energy for a combined Cs/Cu(001) system with the Cs adatom and Cu(001) film greatly separated such that no chemisorption occurs, $E_{\text{band}}(\text{adsorbed})$ is the band energy for the adsorbed Cs/Cu(001) system, $\Delta D = \text{DOS}(\text{unadsorbed}) - \text{DOS}(\text{adsorbed})$ is the difference in the electronic DOSs between the unadsorbed and adsorbed Cs/Cu(001) systems. As

the film thickness changes, the energy levels of the QW states shift. Whenever a QW state crosses the Fermi level from above, it adds energy to E_{band} (unadsorbed) and adds electronic density to unadsorbed $D(E_F)$. Whereas E_{band} (adsorbed) decreases upon the crossing between the QW states and the Fermi level because, as mentioned above, the Cs-Cu orbital hybridization shifts down more in energy by increase of $D(E_F)$. Thus the net consequence is an antiphase oscillation mode of the adsorption energy with respect to the oscillation mode of $D(E_F)$ as a function of the film thickness.

The Cs adsorbate height is plotted in Fig. 10(b) as a function of the film thickness, which also shows the periodic oscillations indicative of the QSE. Compared to the features in the thickness dependence of binding energy, one can see that oscillations in the adsorbate height are very weak and the periods are not easily resolved. This suggests that the adsorbate height is relatively insensitive to the variation of the film thickness and therefore cannot be reliably used to verify the QSE of the ultrathin metal films.

Moreover, we have also calculated the work function of Cs/Cu(001) as a function of the film thickness. The results are shown in Fig. 6(a) (open squares). Compared to the case of clean Cu(001) films, the work function is decreased by a typical value of 2.2 eV [see Fig. 6(b) for the ten-layer case]. Also, the adsorbed work function oscillates with increase of the film thickness. However, one can see that the oscillation mode is different from that without adsorption, and also the oscillating amplitude becomes very weak. This implies that the QW states are different for clean and cesiated Cu(001) thin films. As a result, there no longer exists a simple one-to-one correspondence between the adsorbed QW states and the bulk Cu Fermi surface. More detailed work will be done on this issue.

VI. CONCLUSION

In summary, clean and cesiated Cu(001) thin films have been extensively studied by density-functional theory pseudopotential plane-wave calculations. The dependence of electronic structure, surface energetics, and interlayer relax-

ation upon the thickness of the film has been fully investigated, and clearly shows the metallic QSEs of the film. These QSEs have been shown to be closely related to the occurrence of QW states at the Fermi level. The Fermi surface of bulk Cu is characterized by multiple stationary extrema such as the belly and neck points. As a consequence, the Cu(001) QW states also display the abundant properties at these surface-projected k extrema. For example, we have shown that different film-thickness oscillation modes by calculating the energies of QW states in correspondence with these stationary extrema. Due to the interference between these two kinds of QW states, the energetics and the stability (Fig. 5) of the Cu(001) thin films have been shown in a consistent way to display a quantum beating behavior as a function of the film thickness, with the oscillation periods consisting of long and short length scales. In addition, the calculated energy gap between the highest occupied QW state and lowest unoccupied QW state, which can be directly measured via the STS technique, has been shown to display different slopes and kinks at these extrema in bulk BZ.

We have also extensively discussed another highly interesting issue, i.e., the oscillatory QSEs in surface chemical reactivities, via studying the Cs adsorption on Cu(001) thin films. Through systematic calculations, we have shown that the Cu(001) surface chemical catalysis for Cs adsorption can be uniquely modulated and controlled by the occurrence of QW states at the Fermi level. The Cs adsorption energy and the work function after cesiation show quantum oscillations as a function of the film thickness. The amplitudes in these oscillations reach a typical value of 40 meV. From the application point of view, this result is quite intriguing because 1 ML change in the film thickness can cause an effect equivalent to a temperature change as high as 400 K. These calculated results thus may be used as a guide to tailor catalysis, chemical reactions, and other surface processes in nanostructured materials.

ACKNOWLEDGMENTS

This work was partially supported by the CNSF under Grants No. 10544004 and No. 10604010.

*Corresponding author. zhang_ping@iapcm.ac.cn

¹J. J. Paggel, T. Miller, and T.-C. Chiang, *Science* **283**, 1709 (1999).

²Z. Tesanovic, M. V. Jaric, and S. Maekawa, *Phys. Rev. Lett.* **57**, 2760 (1986).

³A. E. Meyerovich and S. Stepaniants, *Phys. Rev. Lett.* **73**, 316 (1994).

⁴A. Kawabata, *J. Phys. Soc. Jpn.* **62**, 3988 (1993).

⁵T.-C. Chiang, *Surf. Sci. Rep.* **39**, 181 (2000).

⁶M. Milun, P. Pervan, and D. P. Woodruff, *Rep. Prog. Phys.* **65**, 99 (2002).

⁷M. Hupalo, S. Kremmer, V. Yeh, L. Berbil-Bautista, and M. C. Tringides, *Surf. Sci.* **493**, 526 (2001); M. Hupalo and M. C.

Tringides, *Phys. Rev. B* **65**, 115406 (2002).

⁸W. B. Su, S. H. Chang, W. B. Jian, C. S. Chang, L. J. Chen, and T. T. Tsong, *Phys. Rev. Lett.* **86**, 5116 (2001).

⁹R. Otero, A. L. Vázquez de Parga, and R. Miranda, *Phys. Rev. B* **66**, 115401 (2002).

¹⁰H. Hong, C. M. Wei, M. Y. Chou, Z. Wu, L. Basile, H. Chen, M. Holt, and T.-C. Chiang, *Phys. Rev. Lett.* **90**, 076104 (2003).

¹¹D.-A. Luh, T. Miller, J. J. Paggel, M. Y. Chou, and T.-C. Chiang, *Science* **292**, 1131 (2001).

¹²For a review, see Z. Q. Qiu and N. V. Smith, *J. Phys.: Condens. Matter* **14**, R169 (2002), and references therein.

¹³M. N. Baibich, J. M. Broto, A. Fert, F. Nguyen Van Dau, F. Petroff, P. Etienne, G. Creuzet, A. Friederich, and J. Chazelas,

- Phys. Rev. Lett. **61**, 2472 (1988).
- ¹⁴J. E. Ortega and F. J. Himpsel, Phys. Rev. Lett. **69**, 844 (1992).
 - ¹⁵P. Bruno, J. Magn. Magn. Mater. **121**, 248 (1993).
 - ¹⁶D. M. Edwards, J. Mathon, R. B. Muniz, and M. S. Phan, Phys. Rev. Lett. **67**, 493 (1991).
 - ¹⁷Y. Guo, Y.-F. Zhang, X.-Y. Bao, T.-Z. Han, Z. Tang, L.-X. Zhang, W.-G. Zhu, E. G. Wang, Q. Niu, Z. Q. Qiu, J.-F. Jia, Z.-X. Zhao, and Q.-K. Xue, Science **306**, 1915 (2004).
 - ¹⁸Y.-F. Zhang, J.-F. Jia, T.-Z. Han, Z. Tang, Q.-T. Shen, Y. Guo, Z. Q. Qiu, and Q.-K. Xue, Phys. Rev. Lett. **95**, 096802 (2005).
 - ¹⁹M. Kralj, A. Šiber, P. Pervan, M. Milun, T. Valla, P. D. Johnson, and D. P. Woodruff, Phys. Rev. B **64**, 085411 (2001).
 - ²⁰See, for example, S. Å. Lindgren and L. Walldén, Phys. Rev. Lett. **59**, 3003 (1987).
 - ²¹N. V. Smith, N. B. Brookes, Y. Chang, and P. D. Johnson, Phys. Rev. B **49**, 332 (1994).
 - ²²V. L. Moruzzi, J. F. Janak, and A. R. Williams, *Calculated Electronic Properties of Metals* (Pergamon, New York, 1978).
 - ²³Y. Wang, Z.-Y. Lu, X.-G. Zhang, and X. F. Han, Phys. Rev. Lett. **97**, 087210 (2006).
 - ²⁴P. J. Feibelman, Phys. Rev. B **27**, 1991 (1983).
 - ²⁵A. Kiejna, J. Peisert, and P. Schraroch, Surf. Sci. **432**, 54 (1999).
 - ²⁶S. Ciraci and I. P. Batra, Phys. Rev. B **33**, 4294 (1985); I. P. Batra, S. Ciraci, G. P. Srivastava, J. S. Nelson, and C. Y. Fong, *ibid.* **34**, 8246 (1986).
 - ²⁷J. C. Boettger and S. B. Trickey, Phys. Rev. B **45**, 1363 (1992); U. Birkenheuer, J. C. Boettger, and N. Rösch, Chem. Phys. Lett. **341**, 103 (1995); K. F. Wojciechowski and H. Bogdanów, Surf. Sci. **397**, 53 (1998); K. Doll, N. M. Harrison, and V. R. Saunders, J. Phys.: Condens. Matter **11**, 5007 (1999).
 - ²⁸J. M. Carlsson and B. Hellsing, Phys. Rev. B **61**, 13973 (2000).
 - ²⁹C. M. Wei and M. Y. Chou, Phys. Rev. B **66**, 233408 (2002).
 - ³⁰C. M. Wei and M. Y. Chou, Phys. Rev. B **68**, 125406 (2003).
 - ³¹P. Lazić, Ž. Crljen, and R. Brako, Phys. Rev. B **71**, 155402 (2005).
 - ³²D. Yu, M. Scheffler, and M. Persson, Phys. Rev. B **74**, 113401 (2006).
 - ³³A. Ayuela, E. Ogando, and N. Zabala, Phys. Rev. B **75**, 153403 (2007).
 - ³⁴D.-J. Huang, P. D. Johnson, and X. Shi, Phys. Rev. B **54**, 17123 (1996).
 - ³⁵F. G. Curti, A. Danese, and R. A. Bartynski, Phys. Rev. Lett. **80**, 2213 (1998).
 - ³⁶R. Kläsger, D. Schmitz, C. Carbone, W. Eberhardt, P. Lang, R. Zeller, and P. H. Dederichs, Phys. Rev. B **57**, R696 (1998).
 - ³⁷R. K. Kawakami, E. Rotenberg, and Ernesto J. Escorcia-Aparicio, Phys. Rev. Lett. **82**, 4098 (1999).
 - ³⁸Y. Z. Wu, C. Y. Won, E. Rotenberg, H. W. Zhao, F. Toyoma, N. V. Smith, and Z. Q. Qiu, Phys. Rev. B **66**, 245418 (2002).
 - ³⁹A. Danese and R. A. Bartynski, Phys. Rev. B **65**, 174419 (2002).
 - ⁴⁰J. M. An, D. Raczkowski, Y. Z. Wu, C. Y. Won, L. W. Wang, A. Canning, M. A. Van Hove, E. Rotenberg, and Z. Q. Qiu, Phys. Rev. B **68**, 045419 (2003).
 - ⁴¹Y. Z. Wu, A. K. Schmid, M. S. Altman, X. F. Jin, and Z. Q. Qiu, Phys. Rev. Lett. **94**, 027201 (2005).
 - ⁴²Eli Rotenberg, Y. Z. Wu, J. M. An, M. A. Van Hove, A. Canning, L. W. Wang, and Z. Q. Qiu, Phys. Rev. B **73**, 075426 (2006).
 - ⁴³Y. Z. Wu, C. Won, E. Rotenberg, H. W. Zhao, Q.-K. Xue, W. Kim, T. L. Owens, N. V. Smith, and Z. Q. Qiu, Phys. Rev. B **73**, 125333 (2006).
 - ⁴⁴W. L. Ling, Eli Rotenberg, H. J. Choi, J. H. Wolfe, F. Toyama, S. Paik, N. V. Smith, and Z. Q. Qiu, Phys. Rev. B **65**, 113406 (2002).
 - ⁴⁵C. Baldacchini, L. Chiodo, F. Allegretti, C. Mariani, M. G. Betti, P. Monachesi, and R. Del Sole, Phys. Rev. B **68**, 195109 (2003).
 - ⁴⁶F. Bisio, M. Nývlt, J. Franta, H. Petek, and J. Kirschner, Phys. Rev. Lett. **96**, 087601 (2006).
 - ⁴⁷M. Bauer, S. Pawlik, and M. Aeschlimann, Phys. Rev. B **55**, 10040 (1997).
 - ⁴⁸S. Ogawa, H. Nagano, and H. Petek, Phys. Rev. Lett. **82**, 1931 (1999).
 - ⁴⁹A. G. Borisov, J. P. Gauyacq, A. K. Kazansky, E. V. Chulkov, V. M. Silkin, and P. M. Echenique, Phys. Rev. Lett. **86**, 488 (2001).
 - ⁵⁰J. P. Gauyacq, A. G. Borisov, and A. K. Kazansky, Appl. Phys. A: Mater. Sci. Process. **78**, 141 (2004).
 - ⁵¹C. Corriol, V. M. Silkin, D. Sanchez-Portal, A. Arnau, E. V. Chulkov, P. M. Echenique, T. von Hofe, J. Kliever, J. Kröger, and R. Berndt, Phys. Rev. Lett. **95**, 176802 (2005).
 - ⁵²Th. von Hofe, J. Kröger, and R. Berndt, arXiv:cond-mat/0603551.
 - ⁵³D. V. Chudinov, S. E. Kul'kova, and I. Yu. Smolin, Phys. Solid State **45**, 590 (2003).
 - ⁵⁴R.-Q. Wu and D.-S. Wang, Phys. Rev. B **41**, 12541 (1990).
 - ⁵⁵K. Wandelt, in *Physics and Chemistry of Alkali Metal Adsorption*, edited by H. P. Bonzel, A. M. Bradshaw, and G. Ertl (Elsevier, Amsterdam, 1989).
 - ⁵⁶L. Aballe, A. Barinov, A. Locatelli, S. Heun, and M. Kiskinova, Phys. Rev. Lett. **93**, 196103 (2004).
 - ⁵⁷X. Ma, P. Jiang, Y. Qi, J. Jia, Y. Yang, W. Duan, W.-X. Li, X. Bao, S. B. Zhang, and Q.-K. Xue, Proc. Natl. Acad. Sci. U.S.A. **104**, 9204 (2007).
 - ⁵⁸Y. Z. Wu (private communication).
 - ⁵⁹G. Kresse and J. Furthmüller, Phys. Rev. B **54**, 11169 (1996).
 - ⁶⁰G. Kresse and D. Joubert, Phys. Rev. B **59**, 1758 (1999).
 - ⁶¹H. J. Monkhorst and J. D. Pack, Phys. Rev. B **13**, 5188 (1976).
 - ⁶²C. Kittel, *Introduction to Solid State Physics*, 5th ed. (Wiley, New York, 1976).
 - ⁶³R. K. Kawakami, E. Rotenberg, E. J. Escorcia-Aparicio, H. J. Choi, T. R. Cummins, J. G. Tobin, N. V. Smith, and Z. Q. Qiu, Phys. Rev. Lett. **80**, 1754 (1998).
 - ⁶⁴P. M. Echenique and J. B. Pendry, J. Phys. C **11**, 2065 (1978).
 - ⁶⁵N. V. Smith, Phys. Rev. B **32**, 3549 (1985).
 - ⁶⁶E. G. McRae and M. L. Kane, Surf. Sci. **108**, 435 (1981).
 - ⁶⁷V. Fiorentini and M. Methfessel, J. Phys.: Condens. Matter **8**, 6525 (1996).
 - ⁶⁸Z. Y. Zhang, Q. Niu, and C. K. Shih, Phys. Rev. Lett. **80**, 5381 (1998).
 - ⁶⁹Note that the first derivative of the total energy has also been successfully used to study the stability of nanostructures.
 - ⁷⁰H.-R. Tang, W.-N. Wang, and K.-N. Fan, Chem. Phys. Lett. **355**, 410 (2002).
 - ⁷¹J. J. Paggel, C. M. Wei, M. Y. Chou, D.-A. Luh, T. Miller, and T.-C. Chiang, Phys. Rev. B **66**, 233403 (2002).
 - ⁷²Juarez L. F. Da Silva, K. Schroeder, and S. Blügel, Phys. Rev. B **69**, 245411 (2004).
 - ⁷³A. G. Danese, F. G. Curti, and R. A. Bartynski, Phys. Rev. B **70**, 165420 (2004).
 - ⁷⁴W. Berndt, D. Weick, C. Stampfl, A. M. Bradshaw, and M. Scheer, Surf. Sci. **330**, 182 (1995).
 - ⁷⁵S. Andersson and J. B. Pendry, Solid State Commun. **16**, 563

- (1975).
- ⁷⁶J. E. Demuth, D. W. Jepsen, and P. M. Marcus, *J. Phys. C* **8**, L25 (1975).
- ⁷⁷C. von Eggeling, G. Schmidt, G. Besold, L. Hammer, K. Heinz, and K. Müller, *Surf. Sci.* **221**, 11 (1989).
- ⁷⁸S. Aminpirooz, A. Schmalz, L. Becker, N. Pangher, J. Haase, M. M. Nielsen, D. R. Batchelor, E. Bøgh, and D. L. Adams, *Phys. Rev. B* **46**, 15594 (1992).
- ⁷⁹U. Muschiol, P. Bayer, K. Heinz, W. Oed, and J. B. Pendry, *Surf. Sci.* **275**, 185 (1992).
- ⁸⁰S. Mizuno, H. Tochiwara, and T. Kawamura, *Surf. Sci.* **293**, 239 (1993).
- ⁸¹D. A. Arena, F. G. Curti, and R. A. Bartynski, *Phys. Rev. B* **56**, 15404 (1997).
- ⁸²E. Wimmer, A. J. Freeman, J. R. Hiskes, and A. M. Karo, *Phys. Rev. B* **28**, 3074 (1983).
- ⁸³P. Nordlander and J. C. Tully, *Phys. Rev. B* **42**, 5564 (1990).
- ⁸⁴H. Ishida, *Phys. Rev. B* **38**, 8006 (1988); H. Ishida and A. Lieb-sch, *ibid.* **45**, 6171 (1992).
- ⁸⁵D. M. Newns, *Phys. Rev.* **178**, 1123 (1969).
- ⁸⁶J. K. Norskov, *Rep. Prog. Phys.* **53**, 1253 (1990).